ISSN: 2277-3754
ISO 9001:2008 Certified
International Journal of Engineering and Innovative Technology (IJEIT)
Volume 8, Issue 7, January 2019

Simulation of Forced mixed convection for a heat source with a porous baffle in pulsating vertical channel flow

Po-Chuan Huang [a], Chien-Cheng Hung [b]

[a] Department of Energy and Refrigerating Air-Conditioning Engineering, National Taipei University of Technology, Taipei, Taiwan 106, ROC

[b] Department of Energy and Refrigerating Air-Conditioning Engineering, National Taipei University of Technology, Taipei, Taiwan 106, ROC

Abstract: ***This present attempts to use less porous material as a baffle to enhance heat transfer and tries to improve performance further in the pulsating flow instead of the steady flow, i.e. to investigate the heat transfer effect under both of active and passive flow field. This study details the effects of variations in the Darcy number, Strouhal number and oscillating amplitude. The results show excellent heat transfer enhancement with a porous baffle under a pulsating flow than that without baffle in the steady flow. Porous media were widely used as heat sinks in industrial application for the purpose of heat transfer enhancement. Porous media are often mounted on heat sources directly, but much porous materials shall be spent, and both of cost and pressure drop will increase simultaneously. This study analyzes numerically for the pulsating forced convection in a vertical channel with a single porous baffle. The flow field is governed by Navier-Stokes equations in the fluid region, by Darcy-Brinkman-Forchheimer equations in the porous region. Buoyancy force is modeled in the momentum equation for the flow field.***

Keywords: **Mixed convection, Porous foam, pulsating flow.**

I. BACKGROUND/ OBJECTIVES AND GOALS

By early this century, microprocessor scaling has consistently adhered to Moore's law. Thermal Design Power (TDP) rises linearly up to approximately the year 2009~2010 and will remain approximately constant afterwards [1] [2]. Because of the complexity of microprocessor design, there is a possibility of increased local power densities, leading to highly non-uniform heat generation that will cause localized hotspots. The thermal design for cooling microprocessor package has become increasingly challenging, and new cooling technologies are needed for future packages in order to ensure device performance and reliability. Different methods and materials were explored in the recent years. Porous media may be selected as potential candidates for the heat transfer enhancement in the electronic industry.

Porous media have been used very widely in the industry for heat transfer enhancement and energy storage purpose such as catalytic reactors, absorption and adsorption operations, packed bed heat storage units [3], solidification processes, thermal insulation engineering, water movements, nuclear waste repository, heat pipes and heat exchangers [4], regenerators [5], heat sinks in the heat transfer enhancement of electronic components or others [6] [7] [8] [9]. The mechanisms of porous media that contribute to enhance heat transfer are: (1) The channel effect and the mixing effect occurs in the flow field, the former effect causes higher velocities near wall surfaces in the porous medium region and the rear effect produces full

Manuscript received: 22 December 2018
Manuscript received in revised form: 19 January 2019
Manuscript accepted: 04 February 2019
Manuscript Available online: 10 February 2019

ISSN: 2277-3754
ISO 9001:2008 Certified
International Journal of Engineering and Innovative Technology (IJEIT)
Volume 8, Issue 7, January 2019

energy exchange between porous media and pure fluid because of the vortex occurrence and the streamlines distortion in the interface region. P.C. Huang explained the heat transfer enhancement because of the results of four interrelated effects including penetrating effect, blowing effect, suction effect and the effect of boundary layer separation and reattachment [10]. (2) The higher thermal effective conductivity (k_{eff}) in porous matrix contributes to enhance heat transfer in the thermal field due to the solid conductivity (k_s) is often higher than the fluid conductivity (k_f) [11] [12].

Oscillatory-flow heat transfer can be grouped into two categories, pulsating flow and reciprocating flow, and has more stringent time and spatial resolution requirements than steady flow. Pulsating flows are always unidirectional compared with reciprocating flow and can be decomposed into steady and unsteady components, such as in the analytical study of Siegel [13]. Pulsating flow is finding more engineering applications, for example, membrane driven micro-pumps and peristaltic micro-mixers, novel heat exchanger devices for electronic cooling…etc.. Some experimental, numerical and analytical studies on pulsating flow heat transfer can be found in the literature. For high-frequency oscillations in a full developed channel, the effect of the velocity oscillations is sufficiently small that it is not of practical significance. When frequency parameter is low, the velocity profiles resemble much of the quasi-steady solutions, when frequency parameter is large, the effect of oscillation are confined to a narrow zone adjacent to the walls. The effects of pulsating on Nu are pronounced for large pulsation amplitudes and at high pulsation frequencies changes in Nu are generally minor [14] [13]. Heat transfer effect in a tub with pulsating flow was studied analytically by Moschandreou [15], the results indicate that there is a positive peak in a range of moderate frequency values and the Nu is increased, but the effect is reversed when the frequency is outside this range. A numerical study was carried out in pulsating channel flow with two heated block by Kim [16], the results indicate that the flow pulsation can be utilized to enhance heat transport in thermal system. The recirculation flows behind the down system block as well as inside the inter-block region has a strong influence on the thermal transport. In the comparison with a steady flow, the heat transfer enhancement factor of Nu increase up to 21% in the case of Re=500 and St=0.8. The effect of pulsating flow was experimentally investigated from a heated block array inside a channel by Moon [17], a pulsating flow is imposed by an acoustic woofer in this experiment, the results shows that thermal transport from the blocks is greatly affected by the frequency, the amplitude, the inter-block spacing and Reynolds number.

The baffle application to enhance heat transfer can be also found in the literature. Sung [18] studied numerically the force convection effects on different models partially filled with a porous medium in a steady flow horizontal channel. In a model of porous block mounted on the top plate and heat source on the bottom plate, he found that the flow in concentrated to the unobstructed opening and a strong velocity gradient is creased in vicinity of the lower surface of the channel. This point to a vigorous convection near the heat source leads to enhance heat transfer between the heat source and fluid. Chang [19] numerically investigated the effect of a strip solid baffle on the opposing mixed convection in the pulsating flow, the results show that the channel with both flow pulsating and a baffle gives the best heat transfer, maximum Nu occurs at some specific imposed pulsating frequencies which can be considered to be the natural frequency of the system. The steady or pulsating conditions do not affect Nu significantly without baffle.

It is conceivable that synthetic effects combining with the passive effect by porous media and the active effect by pulsating flows can provide a better heat transfer enhancement. The heat transfer researches about the pulsating flow in a full porous channel can be found in the

ISSN: 2277-3754
ISO 9001:2008 Certified
International Journal of Engineering and Innovative Technology (IJEIT)
Volume 8, Issue 7, January 2019

former literature [20], but the synthetic heat transfer effect of a porous baffle in a pulsating and mixed flow has rarely been studied. This paper attempts to use less porous material as a baffle to change the flow field structure for heat transfer enhancement and tries to improve performance further in the pulsating flow instead of the steady flow. The purpose of this study is to investigate the heat transfer effect under both of active and passive flows, and to provide the qualitative analysis and useful conclusions for the industrial thermal design.

II. METHODS

The schematic of the physical model and coordinate system is shown in Fig.1. (a). It includes flow through a vertical channel of a heated source on the left plate and a single porous baffle mounted on the right plate. The heat flux within the heat source is assumed to be equal and other channel walls are insulated. The low temperature fluid enters the channel at uniform temperature T_0 and a pulsating inlet velocity at bottom inlet, then the high temperature fluid exits from top outlet. The major assumptions and simplifications employed in this study are:

(1) The flow is assumed to be unsteady two-dimensional, laminar, incompressible flow.

(2) Gravity is negligible.

(3)The thermo physical properties of the fluid and the porous matrix are assumed to be constant.

(4) The porous matrix is assumed to have uniform porosity and to be isotropic.

(5) The fluid-saturated porous medium is considered homogeneous, isotropic and in local thermodynamic equilibrium (LTE) with the fluid.

III. RESULTS

From the results of this numerical simulation, the heat transfer effect decreases with increasing Da number of porous foam. For the pulsating flow with porous foam, the heat transfer rate is better than steady flow with porous foam or without porous foam. The results of the present work can be considered as an augment heat transfer tool for cooling electric devices.

The Darcy number, $Da=K/R^2$, is directly related to the permeability of the porous medium. To investigate the effect of Darcy number in the pulsating flow, computations were carried out at Re=250, St=0.2, A=0.5&0.8, Gr/Re^2 =1 with $Da=5\times10^{-5}\sim\infty$, respectively. The Nu_m ratio to the values of steady nonporous for at different Darcy numbers are shown in Fig. 6.(a) to represent the heat transfer enhancement. To compare the heat transfer enhancement between the steady and pulsating flow in the high Darcy number range ($Da=3\times10^{-4}\sim\infty$), the curve trend of Nu_m ratio is similar to that in the steady flow. But the Nu_m ratio as the enhancement factor is increased as Darcy number decreases in the low Darcy number range ($Da<3\times10^{-4}$), for example The Nu_m ratio is 1.37 for $Da=3\times10^{-4}$, 1.59 for $Da=1\times10^{-4}$ and 1.64 for $Da=5\times10^{-5}$. This may be explained that the heat transfer enhancement increase due to higher permeability produces severe distortion on flow field and that accompanies with the better mixing effect between the heat source and the low temperature fluid. Fig. 6.(b) also shows the increasing Da increases the velocity u^* transient responses largely to enhance heat transfer on the front section at location (1.0, 0.9) and the transient velocity is similar for all on the rear section at location (4.0, 0.9).

The effect of variations in the Strouhal number and oscillating amplitude is depicted in Fig. 7 for at Re=250, $Da=1\times10^{-4}$, Gr/Re^2=1 with St=0.2~1.6 at A=0.5 and with A=0.2~0.8 at St=0.2, respectively. To compare the mean Nusselt numbers in Fig. 7.(a), the smallest Nu_m appear in the cases of no baffle & steady flow, then in the cases of with baffle & steady flow. The larger Nu_m all appear in the cases of with baffle & pulsating flow and the different Nu_m appear under different oscillating frequencies and amplitudes. As St increases, the Nu_m increases to a critical St value, then decreases up to St=0.8, the Nu_m no change too much at St=0.8~1.6. This result shows no regular rule in the effect of Strouhal number. The

ISSN: 2277-3754
ISO 9001:2008 Certified
International Journal of Engineering and Innovative Technology (IJEIT)
Volume 8, Issue 7, January 2019

increasing *A* increases the Nu_m regularly. This result shows that it's very helpfully to enhance heat transfer in increasing the oscillating amplitude. The case of *A*=0.8 is shown to be the best case with a porous baffle. The Nu_m increase 59% than that in steady nonporous case to present the excellent heat transfer enhancement combining with active (pulsating flow) and passive (porous media) heat transfer. The same conclusion, gained in Chang and Shiau [18], is that a situation with a larger *St* does not imply a higher heat transfer, but the heat transfer increases with a greater pulsating magnitude A. Fig. 7.(b) shows the increasing *A* increases the velocity u^* transient responses largely to enhance heat transfer along the heat source. The current numerical study shows that Nu_m in *A*=0.8 is 1.24 times to that in *A*=0.2 in the case with baffle in the pulsating flow.

A. *Formula and equation*

The "local volume averaging" conservation equations have been derived by Vafai and Tien [21], this technique is used in developing the governing equations in the region of porous matrix for this study. The flow is modeled by the Darcy–Brinkman–Forchheimer equations [22] in the porous matrix to incorporate the viscous and inertial effects and by Navier–Stokes equations [23] in the fluid domain, and the thermal field by the energy equation. Then, an efficient alternative method for combining these sets of governing equations for the fluid and porous regions into one set of conservation equations is to model the whole fluid/porous composite system as a single domain governed by one set of conservations, the solution of which satisfies the matching conditions at both fluid/porous interfaces. The above-mentioned resulting momentum and energy equations are expressed as followings:

1. Governing equations in the fluid domain Continuity equation for fluid:

$$\nabla \bullet \vec{V} = 0 \tag{1}$$

Momentum equations for fluid:

$$\left[\frac{\partial \vec{V}}{\partial t} + (\vec{V} \bullet \nabla)\vec{V}\right] = -\frac{1}{\rho_f}\nabla P + \nu_f \nabla^2 \vec{V} + \vec{g}\beta(T_f - T_0) \tag{2}$$

Energy equation for fluid:

$$\frac{\partial T}{\partial t} + \vec{V} \bullet \nabla T = \alpha_f \nabla^2 T \tag{3}$$

2. Governing equations in the porous medium domain Continuity equation for porous medium:

$$\nabla \bullet <\vec{V}> = 0 \tag{4}$$

Momentum equations for porous medium:

$$\frac{1}{\varepsilon}\left[\frac{\partial <\vec{V}>}{\partial t} + (<\vec{V}> \bullet \nabla)<\vec{V}>\right] = -\frac{1}{\rho_f}\nabla P + \frac{1}{\varepsilon}\nu_{eff}\nabla^2 <\vec{V}> - \left[\frac{\nu_f}{K} + \frac{\varepsilon F}{\sqrt{K}}\left|<\vec{V}>\right|\right]<\vec{V}> + \vec{g}\beta(T - T_0) \tag{5}$$

Energy equation for porous medium:

$$(\rho Cp)_{eff}\frac{\partial <T>}{\partial t} + (\rho Cp)_f\left[<\vec{V}> \bullet \nabla <T>\right] = \nabla \bullet \left[k_{eff}\nabla <T>\right] \tag{6}$$

In the above formulations, < > represent the aforementioned volume-averaged quantities. The effective conductivity k_{eff} can be either measured experimentally or estimated from the porosity and the thermal conductivities of the solid and the fluid. The associated initial conditions and boundary conditions necessary to complete the formulation of the present problem are:

1. Initial conditions (t= 0)

$$u = 0, \quad v = 0, \quad T = T_0 \tag{7}$$

2. At the bottom inlet, ($x=0, 0 \leqq y \leqq R, t>0$)

$$u = 6(y^* - y^{*2}) \times u_0\left[1 + A\sin(\omega t)\right], \quad v = 0, \quad T = T_0 \tag{8}$$

3. At the top outlet, ($x=Lt, 0 \leqq y \leqq R, t>0$)

$$\frac{\partial u}{\partial x} = 0, \quad \frac{\partial v}{\partial x} = 0, \quad \frac{\partial T}{\partial x} = 0 \tag{9}$$

4. Along the right plate ($0<x<Lt, y=0, t>0$)

ISSN: 2277-3754
ISO 9001:2008 Certified
International Journal of Engineering and Innovative Technology (IJEIT)
Volume 8, Issue 7, January 2019

$$u = 0, \quad v = 0, \quad \frac{\partial T}{\partial y} = 0 \tag{10}$$

5. Along the left plate ($0 < x < Lt$, $y = R$, $t > 0$)

Without heat source: $u = 0, \quad v = 0, \quad \frac{\partial T}{\partial y} = 0$

With heat source: (11)

$$u = 0, \quad v = 0, \quad q'' = -k_{eff} \frac{\partial T}{\partial y}$$

In addition to these, the three sets of conservation equations are coupled by the following matching conditions at the fluid/porous interfaces:

6. Along the fluid/porous interface (the continuities of the velocity, temperature, and heat flux are satisfied.) [10]

$$< u >_p \Big|_{g(x,y)=0} = u_f \Big|_{g(x,y)=0}, \quad < v >_p \Big|_{g(x,y)=0} =$$

$$< T >_p \Big|_{g(x,y)=0} = T_f \Big|_{g(x,y)=0}, \quad k_{eff} \frac{\partial < T >_p}{\partial n}\Big|_{g(x,y)=0} = k_f \frac{\partial T_f}{\partial n}\Big|_{g(x} \tag{12}$$

where $g(x, y) = 0$ are the curves defining the fluid/porous interfaces, and the derivative with respect to n represents the normal gradients to these curves at any point on the interfaces. For simplifying governing equations, the non-dimension is employed first and stream-function-vorticity transformation method [24] [25] is used to delete pressure term then. All non-dimensionalized variables are based on the following definitions:

$$x^* = \frac{x}{R}, \quad y^* = \frac{y}{R}, \quad Lt^* = \frac{Lt}{R}, \quad W_p^* = \frac{W_p}{R}, \quad H_p^* = \frac{H_p}{R}, \quad x_p^* = \frac{x_p}{R}, \quad L_h^*$$

$$u^* = \frac{u}{u_0}, \quad v^* = \frac{v}{u_0}, \tag{13}$$

$$\left| < \vec{V} > \right| = \sqrt{< u >^2 + < v >^2}$$

$$P^* = \frac{P}{\rho u_0^2}, \quad T^* = \frac{T - T_0}{q'' R / k_f}, \quad t^* = t u_0 / R$$

$$\psi^* = \frac{\psi}{u_0 R}, \quad \zeta^* = \frac{R\zeta}{u_0}$$

Where (x^*, y^*) are dimensionless rectangular Cartesian coordinates, Ψ and ζ are the stream function and vorticity, respectively, which are related to the fluid velocity components u and v by

$$u = \frac{\partial \psi}{\partial y}, \quad v = -\frac{\partial \psi}{\partial x}, \quad \zeta = \frac{\partial v}{\partial x} - \frac{\partial u}{\partial y} \tag{14}$$

The dimensionless governing equations are expressed as followings:

1. Dimensionless governing equations in the fluid domain

Stream function-vorticity transformation for fluid:

$$\frac{\partial^2 \psi^*}{\partial x^{*2}} + \frac{\partial^2 \psi^*}{\partial y^{*2}} = -\zeta^* \tag{15}$$

Momentum equations for fluid:

$$\frac{\partial \zeta^*}{\partial t^*} + u^* \frac{\partial \zeta^*}{\partial x^*} + v^* \frac{\partial \zeta^*}{\partial y^*} = \frac{1}{Re_f}\left[\frac{\partial^2 \zeta^*}{\partial x^{*2}} + \frac{\partial^2 \zeta^*}{\partial y^{*2}}\right] - \frac{Gr}{Re_f^2}\frac{\partial T^*}{\partial y^*} \tag{16}$$

Energy equation for fluid:

$$\frac{\partial T^*}{\partial t^*} + u^* \frac{\partial T^*}{\partial x^*} + v^* \frac{\partial T^*}{\partial y^*} = \frac{1}{Pe_f}\left[\frac{\partial^2 T^*}{\partial x^{*2}} + \frac{\partial^2 T^*}{\partial y^{*2}}\right] \tag{17}$$

2. Dimensionless governing equations in the porous medium domain Stream function-vorticity transformation for porous medium:

$$\frac{\partial^2 \psi_p^*}{\partial x^{*2}} + \frac{\partial^2 \psi_p^*}{\partial y^{*2}} = -\zeta_p^* \tag{18}$$

Momentum equations for porous medium:

$$\frac{\partial \zeta_p^*}{\partial t^*} + u_p^* \frac{\partial \zeta_p^*}{\partial x^*} + v_p^* \frac{\partial \zeta_p^*}{\partial y^*} = \frac{1}{Re_{eff}}\left[\frac{\partial^2 \zeta_p^*}{\partial x^{*2}} + \frac{\partial^2 \zeta_p^*}{\partial y^{*2}}\right] - \frac{\varepsilon}{Re_{eff}\, Da}\zeta_p^*$$
$$- \frac{F\varepsilon^2}{\sqrt{Da}}\left|\vec{V}_p^*\right|\zeta_p^* - \frac{F\varepsilon^2}{\sqrt{Da}}\left[v_p^* \frac{\partial \left|\vec{V}_p^*\right|}{\partial x^*} - u_p^* \frac{\partial \left|\vec{V}_p^*\right|}{\partial y^*}\right] - \varepsilon \frac{Gr}{Re_{eff}^2}\frac{\partial T_p^*}{\partial y^*} \tag{19}$$

Energy equation for porous medium:

ISSN: 2277-3754
ISO 9001:2008 Certified
International Journal of Engineering and Innovative Technology (IJEIT)
Volume 8, Issue 7, January 2019

$$R_c \frac{\partial T_p^*}{\partial t^*} + u_p^* \frac{\partial T_p^*}{\partial x^*} + v_p^* \frac{\partial T_p^*}{\partial y^*} = \frac{R_k}{Pe_f}\left[\frac{\partial^2 T_p^*}{\partial x^{*2}} + \frac{\partial^2 T_p^*}{\partial y^{*2}}\right] \quad (20)$$

The non-dimensional parameters in above-mentioned equations are as followings:

$$Re_f = \frac{u_0 R}{\nu_f}, \quad Pr_f = \frac{\nu_f}{\alpha_f}, \quad Pe_f = \frac{u_0 R}{\alpha_f} = Re_f Pr_f, \quad \alpha_f = \frac{k_f}{\rho C_l}$$

$$Gr = \frac{g\beta q'' R^4}{k_f \nu^2} \quad (21)$$

$$Re_{eff} = \frac{u_0 R}{\nu_{eff}}, \quad Da = \frac{K}{R^2},$$

$$R_c = \frac{(\rho C_p)_{eff}}{(\rho C_p)_f}, \quad R_k = \frac{k_{eff}}{k_f}, \quad S_t = \frac{fR}{u_0}$$

ν_{eff} is almost equal to ν_f from the experiment of Lundgren [26], R_k is the thermal conductivity ratio. Strouhal number S_t is a dimensionless parameter of frequency, the relationship between angular velocity ω and frequency f is $\omega=2\pi f$.

The associated dimensionless initial conditions and boundary conditions necessary to complete the formulation of the present problem are:

1. Initial conditions ($t^*= 0$)

$$u^* = 0, \quad v^* = 0, \quad \psi^* = 0, \quad \zeta^* = 0, \quad T^* = 0 \quad (22)$$

2. At the bottom inlet, ($x^*=0$, $0 \leqq y^* \leqq 1$, $t^* > 0$)

$$u^* = 6\left(y^* - y^{*2}\right) \times \left[1 + A\sin(2\pi S_t t^*)\right], \quad v^* = 0, \quad T^* = 0$$

$$\psi^* = \left(3y^{*2} - 2y^{*3}\right) \times \left[1 + A\sin(2\pi S_t t^*)\right], \quad \zeta^* \quad (23)$$

3. At the top outlet, ($x^*=Lt^*$, $0 \leqq y^* \leqq 1$, $t^* > 0$)

$$\frac{\partial u^*}{\partial x^*} = 0, \quad \frac{\partial v^*}{\partial x^*} = 0, \quad \frac{\partial T^*}{\partial x^*} = 0 \quad (24)$$

$$\frac{\partial^2 \psi^*}{\partial x^{*2}} = 0, \quad \frac{\partial \zeta^*}{\partial x^*} = 0$$

4. Along the right plate ($0 < x^* < Lt^*$, $y^*=0$, $t^* > 0$)

$$u^* = 0, \quad v^* = 0, \quad \frac{\partial T^*}{\partial y^*} = 0$$

$$\psi^* = 0, \quad \zeta^* = -\frac{\partial^2 \psi^*}{\partial y^{*2}} \quad (25)$$

5. Along the left plate ($0 < x^* < Lt^*$, $y^*=1$, $t^* > 0$)

$$u^* = 0, \quad v^* = 0,$$

$$\psi^* = 1 + A\sin(2\pi S_t t^*), \quad \zeta^* = -\frac{\partial^2 \psi^*}{\partial y^{*2}} \quad (26)$$

Without heat source: $\frac{\partial T^*}{\partial y^*} = 0$; With heat source:

$$\frac{\partial T^*}{\partial y^*} = -\frac{1}{R_k}$$

In addition to these, the three sets of conservation equations are coupled by the following matching conditions at the fluid/porous interfaces:

6. Along the fluid/porous interface (the continuities of the velocity, temperature, and heat flux are satisfied.) [10]

$$u_p^* = u_f^*, \quad v_p^* = v_f^*, \quad \psi_p^* = \psi_f^*, \quad \zeta_p^* = \zeta_f^*$$

$$T_p^* = T_f^*, \quad k_{eff} \frac{\partial T_p^*}{\partial n^*} = k_f \frac{\partial T_f^*}{\partial n^*} \quad (27)$$

To assess the effects of the porous media on the heat source heat transfer, the time-local Nusselt number along the surface of heat source is evaluated as follow:

$$Nu_{x,t} = \frac{hR}{k_f} = \frac{-R_k}{T_w^*}\left(\frac{\partial T^*}{\partial y^*}\right)\Big|_{y^*=1} \quad (28)$$

Where $T_w^* = \frac{T_w - T_0}{q'' R / k_f}$ is the dimensionless surface temperature at the heat source?

The overall space-time mean Nusselt number for heat source is calculated as follow:

ISSN: 2277-3754
ISO 9001:2008 Certified
International Journal of Engineering and Innovative Technology (IJEIT)
Volume 8, Issue 7, January 2019

$$Nu_m = \frac{1}{\tau A_i}\int_0^{\tau}\int_0^{A_i} Nu_{x,t}\, dA dt \qquad (29)$$

Where τ and A_i are overall time period and overall surface area for each heat source respectively. The flow separation may occur around the fibers at high velocities, while this leads to a larger pressure-drop, the associated mixing substantially enhances the heat transfer, this implies that a higher driven force is required. In the design of heat sinks or baffles for cooling electronic packaged, the heat removal capability must be assessed together with the driven force required to operate the system i.e. the pumping power. In the stream function-vorticity formulation, the pressure field is eliminated in obtaining the solution. However, the pressure field can be recovered from the converged stream function and vorticity fields by integrating the pressure gradient along the channel wall with the no-slip boundary conditions [10] [24]. The total pressure drop along the left channel wall is then obtained from

$$\Delta P^* = \frac{1}{\tau}\int_0^{\tau}\int_0^{Lt^*}\left|\left(\frac{\partial P^*}{\partial x^*}\right)_{y^*=1}\right| dx^* dt = \frac{1}{\tau}\int_0^{\tau}\int_0^{Lt^*}\left|\left(-\frac{1}{Re}\frac{\partial \zeta^*}{\partial y^*}\right)_{y^*=1}\right| dx^* dt \qquad (30)$$

B. *Figures and Tables*

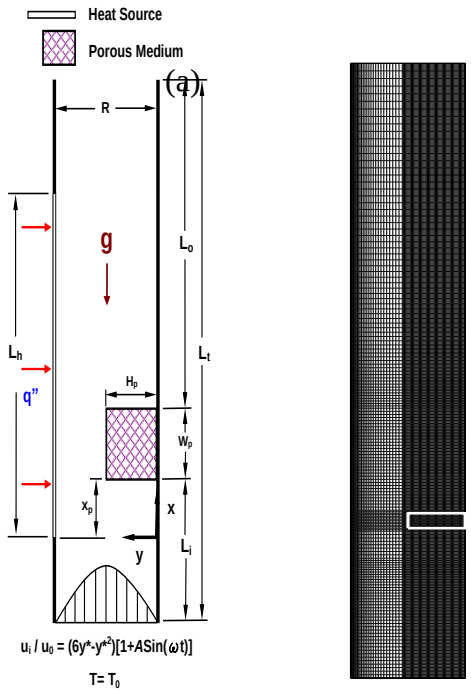

Fig. 1. (a) Schematic diagram of the heated source mounted with porous baffle problem and (b) a typical non-uniform staggered meshed system for the computational domain.

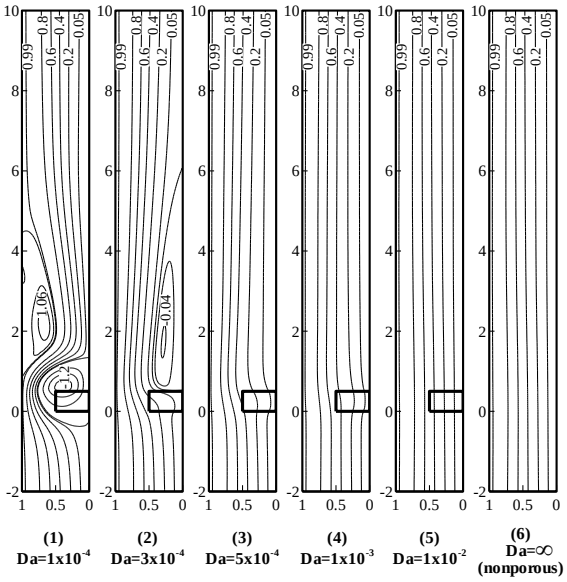

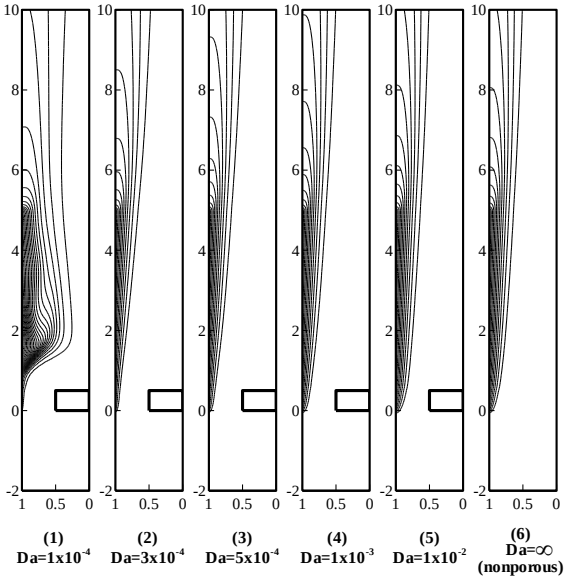

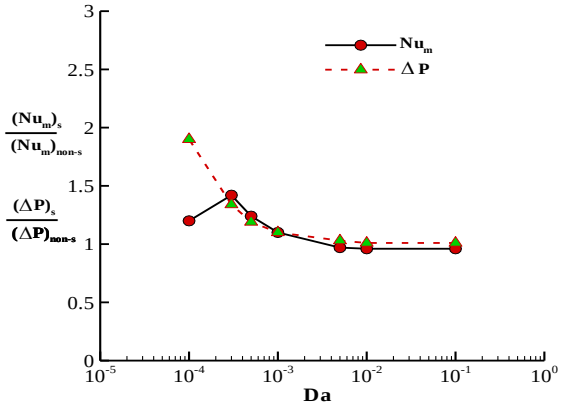

ISSN: 2277-3754
ISO 9001:2008 Certified
International Journal of Engineering and Innovative Technology (IJEIT)
Volume 8, Issue 7, January 2019

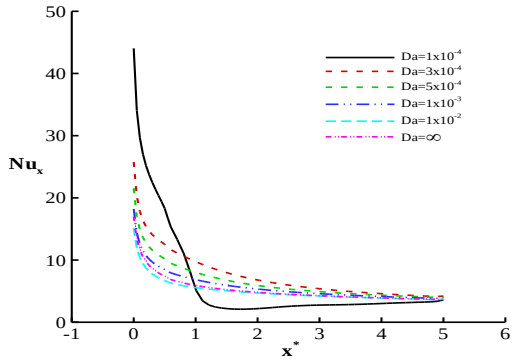

Fig. 2. Effects of Darcy numbers in steady flow on (a) streamlines ($\Delta\Psi$=0.2 for $0 \leqq \Psi \leqq 1$), (b) isotherms (ΔT^*=0.02 for $0 \leqq T^* \leqq 0.5$), (c) the heat transfer enhancement factor $(Nu_m)_s/(Nu_m)_{non\text{-}s}$ and Pressure drop ratio $(\Delta P)_s/(\Delta P)_{non\text{-}s}$ and (d) the local Nesselt number distribution with Re=250, Gr/Re^2=1.0, Pr=0.7.

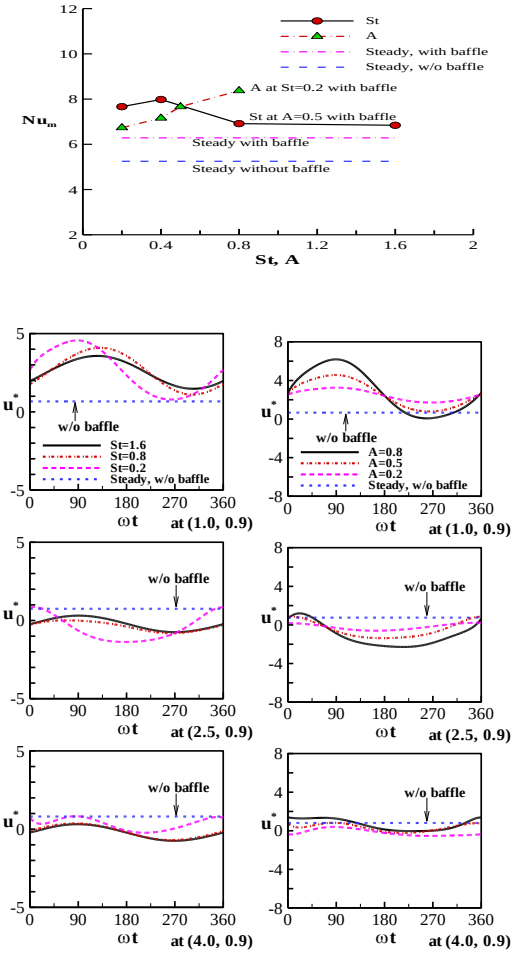

Fig 3. Effect of Strouhl numbers and oscillating amplitude on (a) the mean Nusselt number Nu_m and (b) the velocity u^* transient responses near the left plate with Re=250, Da=1×10^{-4}, Gr/Re^2=1.0.

REFERENCES

[1] R.S. Prashor, J. Chang, I. Sauciuc, S. Narasimhan, D. Chau, G. Chrysler, A. Myers, S. Prstic, C. Hu, Nano and micro technology-based next-generation package-level cooling solutions, Intel Technology Journal 9 (4) (2005) 285-296.

[2] R. Mahajan, R. Nair, V. Wakharkar, J. Swan, J. Tang, G. Vandentop, Emerging directions for packing technologies, Intel Technology Journal 6 (2) (2002) 62-75.

[3] K. Vafai, M. Sozen, "Analysis of energy and momentum transport for fluid flow through a porous bed", Journal of Heat Transfer, Vol. 112, pp. 691–699, 1990.

[4] K. Boomsma, D. Poulikakos, F. Zwick, "Metal foams as compact high performance heat exchangers", Mechanics of Materials, Vol. 35, pp. 1161-1176, 2003.

[5] K. Muralidhar, K. Suzuki, "Analysis of flow and heat transfer in a regenerator mesh using a non-Darcy thermally non-equilibrium model", Int. Journal of Heat and Mass Transfer, Vol. 44, pp. 2493-2504, 2001.

[6] P.C. Huang, K. Vafai, "Analysis of forced convection enhancement in a channel using porous block", Journal of Thermo physics and Mass Transfer, Vol. 8, No.3, pp. 563–573, 1994.

[7] A. Hadim, "Forced Convection in A Porous Channel with Localized Hest Sources", Journal of Heat Transfer, Vol. 116, pp. 465-472, May 1994.

[8] R. Rachedi, S. Chikh, "Enhancement of electronic cooling by insertion of foam materials", Int. Journal of Heat and Mass Transfer, Vol. 37, pp. 371–378, 2001.

[9] S.Y. Kim, Jin Wook Peak, Byung Ha Kang, "Thermal performance of aluminum-foam heat sinks by forced air cooling", IEEE Transactions on Components and Packaging Technologies, Vol. 26, No.1, pp. 262-267, 2003.

[10] P.C. Huang, C.F. Yang, J.J. Huang, M.T. Chiu, "Enhancement of forced-convection cooling of multiple

ISSN: 2277-3754
ISO 9001:2008 Certified
International Journal of Engineering and Innovative Technology (IJEIT)
Volume 8, Issue 7, January 2019

heated blocks in a channel using porous covers", Int. Journal of Heat and Mass Transfer, Vol. 48, pp. 647–664, 2005.

[11] K.C. Leong, L.W. Jin, "Characteristics of oscillating flow through a channel filled with open cell metal foam", Int. Journal of Heat and Fluid Flow, Vol. 27, pp. 144-153, 2006.

[12] Devarakonda Angirasa, "Forced convective heat transfer in metallic fibrous materials", Journal of Heat Transfer, Vol. 124, pp. 739–745, 2000.

[13] R. Siegel, M. Perlmutter, "Heat transfer for pulsating laminar duct flow", Trans. ASME Journal of Heat Transfer, 84(2), pp. 111–123, 1962.

[14] S.Y. Kim, B.H. Kang, J.M. Hyun, "Heat transfer in the thermally developing region of a pulsating channel flow", Int. Journal of Heat and Mass Transfer, Vol. 36, No.17, pp. 4257–4266, 1993.

[15] T. Moschandreou, M. Zamir, "Heat transfer in a tube with pulsating flow and constant heat flux", Int. Journal of Heat and Mass Transfer, Vol. 40, No.10, pp. 2461–2466, 1997.

[16] S.Y. Kim, B.H. Kang, "Forced convection heat transfer from two heated blocks in pulsating channel flow", Int. Journal of Heat and Mass Transfer, Vol. 41, No.3, pp. 625–634, 1998.

[17] J.W. Moon, S.Y. Kim, H.H. Cho, "Frequency-dependent heat transfer enhancement from rectangular heated block array in a pulsating channel flow", Int. Journal of Heat and Mass Transfer, Vol. 48, pp. 4904–4913, 2005.

[18] H.J. Sung, S.Y. Kim, J.M. Hyun, "Force convection from an isolated heat source in a channel with porous medium", Int. Journal of Heat and Fluid Flow, Vol. 16, No.6, pp. 527–535, 1995.

[19] T.S. Chang, Y.H. Kim, Shiau, "Flow Pulsation and baffle's effects on the opposing mixed convection in a vertical channel", Int. Journal of Heat and Mass Transfer, Vol. 48, pp. 4190–4204, 2005.

[20] J.W. Paek, B.H. Kang, J.M. Hyun, "Transient cool-down of a porous medium in pulsating flow", Int. Journal of Heat and Mass Transfer, Vol. 42, pp. 3523–3527, 1999.

[21] K. VAFAI, C. L. TIEN, "Boundary and Inertia Effects on Flow and Heat Transfer in Porous Media", Int. J. Heat Mass Transfer, Vol. 24, pp. 195-203, 1980.

[22] B. Alazmi, K. Vafai, "Analysis of variants within the porous media transport models", Journal of Heat Transfer, Vol. 122, pp. 303–326, 2000.

[23] I. G. Currie, Fundamental Mechanics of Fluids, McGraw-Hill, Inc., 1974.

[24] D.A. Anderson, J.C. Tannehill, R.H. Pletcher, Computational Fluid Mechanics and Heat Transfer, Chapter 5, McGraw-Hill Book Company, 1984.

[25] Roger Peyiet Thomas, D. Taylor, Computational Method for Fluid Flow, Springer-Verlag New York Heidelberg Berlin, 1985.

[26] T.S. Lundgren, "Slow Flow through Stationary Random Beds and Suspensions of Spheres", Journal of Fluid Mech., Vol. 51, pp. 273–299, 1972.